Acta Crystallographica Section D
Biological Crystallography
ISSN 0907-4449

A new highly integrated sample environment for protein crystallography

Lilian Jacquamet,[a] Jeremy Ohana,[a] Jacques Joly,[a] Pierre Legrand,[b] Richard Kahn,[a] Franck Borel,[a] Michel Pirocchi,[a] Philippe Charrault,[a] Philippe Carpentier[a] and Jean-Luc Ferrer[a]*

[a]IBS J.-P. Ebel CEA-CNRS-UJF, 41 Rue Jules Horowitz, 38027 Grenoble CEDEX 1, France, and [b]EMBL-Grenoble, 6 Rue Jules Horowitz, BP 181, 38042 Grenoble CEDEX 9, France

Correspondence e-mail: jean-luc.ferrer@ibs.fr

Received 26 August 2003
Accepted 6 March 2004

Protein crystallography is becoming a popular technique that is routinely used to access structural information. At one end of the process, sample preparation is now facilitated by commercially available crystallization kits. At the other end, structure determination has been made easier by automated software. Data collection, the step in between, is now usually performed on synchrotron sources. However, it is still restricted to experienced users and requires significant help from beamline staff. Part of this difficulty arises from the sophisticated experimental setup, which comprises a goniometer, a magnetic head, a device for changing the sample and monitoring accessories. It was proposed that this setup could be simplified by replacing these elements by a robotic arm that can perform all of the required tasks. In the present paper, it is demonstrated that this new setup can be used on a synchrotron beamline to mount and centre the sample and to collect diffraction data. This new system completely changes the design of the experimental setup by merging functions that were previously considered to be distinct. Moreover, automation of sample handling need not be considered as a specific development and is now included in a unique multipurpose device.

1. Introduction

X-ray crystallography is a widely used technique for providing a three-dimensional representation of molecules in a crystal. Scientists have employed X-ray crystallography to determine the crystal structures of many molecules: 85% of the structures deposited in the Protein Data Bank (http://www.rcsb.org/) were obtained by this method. However, this technique, particularly when applied to challenging biological macromolecule structure determination, requires very specific equipment and highly specialized skills.

A typical X-ray crystallography apparatus is comprised of an X-ray generator (laboratory or synchrotron source), a goniometer on which an accurately adjustable positioning device is mounted (the goniometer head) and a detector. Raw diffraction data collected by the detector are entered into a computer program for processing. In order to perform an X-ray crystallographic analysis, a crystal sample must be mounted onto the positioning device and carefully aligned. X-ray diffraction data are then collected at a number of rotational angles. Because the typical dimensions of the crystals and the diameter of the X-ray beam are in the range from ten to a few hundred micrometres, the alignment requires a high degree of precision. In addition, to ensure the integrity of the crystals, they must be stored in liquid nitrogen and maintained at a temperature close to that of liquid

nitrogen during the entire mounting, alignment and data-collection steps.

Of the four main experimental components (the source, the sample environment, the detector and the data-processing facilities), three have evolved rapidly during the past ten years. Third-generation synchrotron sources now provide such a high-intensity beam that crystals as small as 10 µm can be used for structure determination (Cusack *et al.*, 1998). The low divergence of the beam delivered by synchrotron sources is also an ideal tool for the structural analysis of large molecular assemblies such as viruses (Burroughs *et al.*, 1995). Electronic detectors, such as imaging-plate or CCD-based detectors, have now replaced the film cassette and its off-line reading device. Solid-state detectors will soon be available, integrating the sensitive area and the preamplification stage into the same component. The steps in the structure solution, such as phasing, solvent flattening and model building, are highly automated and can be included in a simple software package (de La Fortelle & Bricogne, 1997; Terwilliger & Berendzen, 1999).

In comparison, the evolution of the sample environment is quite recent. It is the consequence of the emergence of the post-genomics era (Abola *et al.*, 2000), with the development of systematic structure-solution projects (structural genomics projects). In order to face this rapidly growing demand for beam time, it is necessary to improve and facilitate sample handling. As a consequence, remote-controlled goniometer heads are becoming more common and several groups have developed sample changers (Muchmore *et al.*, 2000; Cohen *et al.*, 2002; Earnest *et al.*, 2002), remote-control software (McPhillips *et al.*, 2002) and laboratory information-management systems software (LIMS, see Peat *et al.*, 2002; http://halx.genomics.eu.org) dedicated to X-ray crystallography. So far, these evolutions consist of the addition of new components to an already complicated setup. The new setup we propose consists of a radically simplified and more efficient sample environment for biological macromolecular crystallography. A description of the new sample-handling device we have developed is given below.

2. The classical setup

2.1. Sample mounting

Because they have a large solvent content, usually in the 30–70% range, macromolecular crystals require special treatment compared with crystals of small molecules. These crystals are usually flash-frozen at liquid-nitrogen temperature to prevent them from drying and to minimize possible damage caused by radiation (Teng & Moffat, 1998). The most widely used technique for sample mounting is the loop method: it consists of using a loop to fish out the crystal in the crystallization drop, which is suspended by surface tension in a thin film of cryoprotected buffer. These loops are usually made of various fine (10–50 µm diameter) nylon fibres in order to avoid the absorption and scattering of X-rays.

Table 1
Some existing sample changers for macromolecular crystallography.

Developer	Description	Comments
SSRL (Stanford, USA)	Four-axis arm	On site (Abola *et al.*, 2000)
ALS (Berkeley, USA)	Single-axis transfer	On site
APS (Argone, USA)	Four-axis arm	In development
EMBL Grenoble (France)	Single-axis transfer	In development
FIP-BM30A (France)	Six-axis arm	On site (Ohana *et al.*, 2004)
Rigaku/Abbott Lab. (USA)	Six-axis arm	Commercial (Olson *et al.*, 2002)
MAR Research	Single-axis transfer	Commercial
Bruker (USA)	Single-axis transfer	Commercial

There are several ways of attaching the loop-supporting pin to the positioning device. Two widely used methods are (i) insertion of the pin directly into a hole drilled in the head of the positioning device and (ii) attachment of a magnet to the head of the positioning device, to which a magnetic pin holder is attracted and rigidly held. The pin holder is either screwed into or magnetically attached to a small plastic vial that is placed in liquid nitrogen for storage and transportation. This second method is at present the most widely used and therefore it was standardized.

The manual procedure for mounting the sample consists of transferring the vial into a small Dewar filled with liquid nitrogen. The pin holder is then detached from the vial with the help of dedicated tools and transferred to the head of the positioning device.

In order to face rapidly growing demand, beamlines dedicated to macromolecular crystallography are now being equipped with automated sample changers. These devices range from simple tong translation along a rail to six-axis robots (see Table 1). They allow mounting/unmounting of the sample remotely and rapidly.

2.2. Sample centring

The goniometer head allows precise adjustments along three axes: one axis along the spindle axis and two axes perpendicular to the spindle axis. This goniometer head is used to bring the sample to the intersection of the X-ray beam and the goniometer spindle axis. A video camera allows the display of a magnified image of the sample on a video monitor. Cross-hairs on the video display indicate the desired position of the sample. In order to maintain the sample at a sufficiently low temperature once it is mounted, a cold nitrogen stream is directed towards the sample position.

In most setups, a manual procedure for lining up the sample is often still used: using the video image on the monitor, the operator turns adjustment screws controlling the three axes of corresponding stages until the sample is centred at the intersection of the X-ray beam and the spindle axes (as indicated by the cross-hairs on the video display). Remotely controlled translation stages are becoming more widely used. On some synchrotron beamlines this centring can be performed from the control room using an appropriate graphical computer

Table 2
Some goniometers available on synchrotron beamlines dedicated to macromolecular crystallography.

Synchrotron facility	Beamline	Goniometer geometry
Photon Factory (Japan)	BL-6A	Single-axis + 2θ
Photon Factory (Japan)	BL-18B	Single-axis + 2θ
NSLS (USA)	X8C	Single-axis + 2θ (ADSC)
NSLS (USA)	X9A	Single-axis + 2θ (MAR Research)
NSLS (USA)	X9B	Mini-κ
ESRF (France)	ID9	Three-axis (Eulerian cradle)
ESRF (France)	ID14	Single-axis
ESRF (France)	FIP-BM30A	Three-axis + 2θ

program. However, more frequently the crystallographer has to define the sample position manually because of the difficulty of visualizing the crystal in the loop.

2.3. Sample orientation

Some experimental setups also allow angular adjustments around one or more axes. The sample can then be oriented in the beam according to experimental requirements, by means of head angular adjustments or circles of the goniometer. Complexity of the goniometers can range from simple single-axis to sophisticated four-circle/κ goniometers (see Table 2).

On synchrotron beamlines when the altitude of the beam is not fixed the table where the goniometer is installed must be moved to bring the main axis of the goniometer into the beam.

2.4. Sample rotation

Once the sample has been centred and oriented if necessary, analysis of the sample by X-ray diffraction can begin. The sample is rotated synchronously with the opening of a shutter that allows its controlled exposure to the X-rays beam. The procedure is described in detail by Garman & Schneider (1997).

3. A new experimental setup

A breakthrough in sample handling is only possible if the present approach, as described above, is replaced by a new one with a high degree of integration. Here, we propose a new system that replaces the goniometer, the goniometer head and the sample changer, and possibly the beam monitor, by a single six-axis robot that performs the following functions.

(i) Removes the sample from the storage device (a Dewar, for example).

(ii) Puts it into the beam path.

(iii) Orients the sample if necessary.

(iv) Rotates the sample with respect to the appropriate axis during the exposure time.

(v) Replaces it in the storage container at the end of the data collection.

(vi) Moves monitors or beam-imaging systems into the beam for diagnostic purposes.

We demonstrate here that a robotic arm can be used on a synchrotron beamline for both mounting the sample (Ohana *et al.*, 2004) and collecting diffraction data. This completely changes the way crystallographers picture an experimental setup by merging functions that were previously separate. Until now, it had always been assumed that robotic arms do not possess the required accuracy to perform crystal oscillations. Our tests show that the accuracy of such equipment is sufficient. These results were obtained without any modification of the hardware and the major effort was put into the development of the control software.

Using a single device for all the steps where sample handling is involved, instead of a set of distinct equipment, removes the artificial distinction between some of these steps. Mounting, centring and rotating the sample are now a single operation. A robotic arm brings the sample into the beam and keeps it in that fixed position during the rotation around a given axis. Such a robotic arm can rotate the sample with respect to any axis, even if this axis is not a physical axis of the arm.

This new setup presents many advantages with respect to the systems that were commonly used previously.

(i) A very expensive dedicated goniometer is replaced by a cheap commercial device.

(ii) High reliability: commercial robotic arms are built to work in difficult environments. Moreover, the reduced number of motors contributes to a reduced risk of failure.

(iii) Gain in size: the robotic arm can replace a large goniometer and its sample changer, being capable of orienting the sample and, when used in single-axis geometry, being smaller than a goniometer with the same capabilities.

(iv) Gain in time: no dead time to synchronize equipment.

(v) Flexibility: the new device can be adapted to any experimental geometry. Moreover, it can perform complementary tasks (monitors and beam-imaging system handling).

This new setup may completely change crystallographic experiments. In the future, a large number of devices could be replaced by three components: the sample environment (collimator, beam-stop, on-axis microscope), a robotic arm for sample handling and a detector with a translation/rotation stage (Fig. 1).

4. Detailed description

We have tested this new setup on beamline FIP-BM30A (Roth *et al.*, 2002) at the European Synchrotron Radiation Facility (ESRF, France). We used an RX-60L robot from Stäubli (Faverge, France), but any robotic arm with the required accuracy could be used. This robot, as well as the associated Dewar, were installed on FIP-BM30A to serve as a sample changer (Ohana *et al.*, 2004; Fig. 2). A mechanical goniometer head was mounted at the extremity of the arm with a magnet at its end (Fig. 3). To keep things simple, we used the existing sample environment already installed on our diffractometer, including a microscope and a sample-cryocooling system (Fig. 3). In order to adapt the system to that environment, we extended the arm and set the spindle axis approximately 30° off the perpendicular to the X-ray beam (Fig. 5).

The results obtained are detailed below. They prove that a robot is precise enough for most crystallographic experiments. The setup could be made even more precise by using the standard six-axis arm, which is shorter than the elongated version we tested. Furthermore, better control of the robot could be obtained using commercially available specially designed electronics.

4.1. Technical characterization

The sphere of confusion (the volume to which the centre of rotation is confined during the whole data collection) and the overall positioning repeatability of this system were measured with a needle attached to the end of the arm. The needle displacements were observed with the microscope installed on the four-circle goniometer on FIP-BM30A, with which motions of few micrometres can be appreciated. The following characteristics were determined.

(i) The radius of the sphere of confusion when using the last rotation of the arm as the spindle axis is smaller than 5 µm.

(ii) The radius of the sphere of confusion when using the appropriate combination of rotation to perform a rotation with respect to an arbitrary axis is about 30 µm.

(iii) The repeatability when returning to the recorded beam position is 30 µm, if one axis is moved at a time.

(iv) The same repeatability, when the robot calculates the trajectory, is not measurable (*i.e.* much smaller than 10 µm).

The speed regularity was measured with an ROD 260-18000 Heidenhain coder. The output of the coder was analyzed with an oscilloscope. For a 1° rotation in 10 s with the last axis 15° off the spindle axis (*i.e.* a spindle along a virtual axis), the first 0.01° was recorded in 105 ms instead of 100 ms for the following steps. Assuming a constant acceleration during the acceleration ramp, the acceleration duration is 0.01 s. It demonstrated that the acceleration-ramp length was less than 0.001°. When using only the last axis as a spindle axis, the acceleration-ramp length becomes negligible.

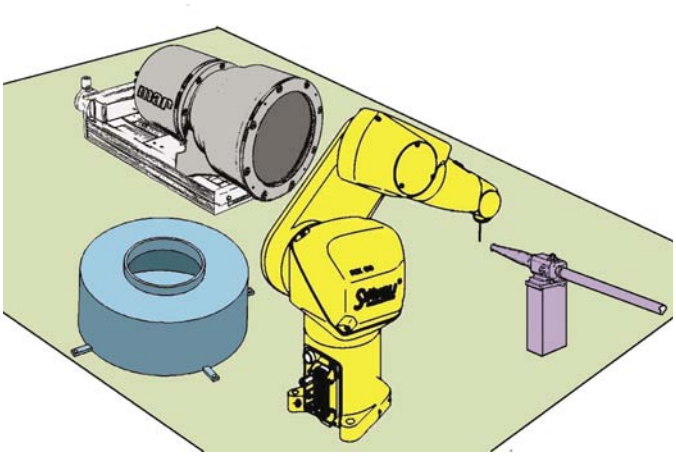

Figure 1
The new integrated experimental environment. Purple, collimator and on-axis microscope; yellow, robotic arm; blue, storage Dewar; grey, detector on a translation/rotation stage.

4.2. Sample viewing and centring

All the tests presented here assume that the sample is centered or at least that its position is sufficiently well defined to place and keep it in an X-ray beam of comparable size. The program that we have developed is based on the analysis of the image obtained with a microscope (Roth *et al.*, 2002). In this image, the sample, which is constituted of the pin and the loop containing the crystal, is isolated from the image background by external contouring. The loop and the crystal are then isolated from the rest of the object by analyzing of the shape of the contour. The larger part of the loop is then centred in the beam. The limitation of this software is that it is the loop and not the sample that is centred. This limitation is a result of the difficulty of viewing the sample, considering that the sample consists of a crystal frozen in a mother-liquor drop

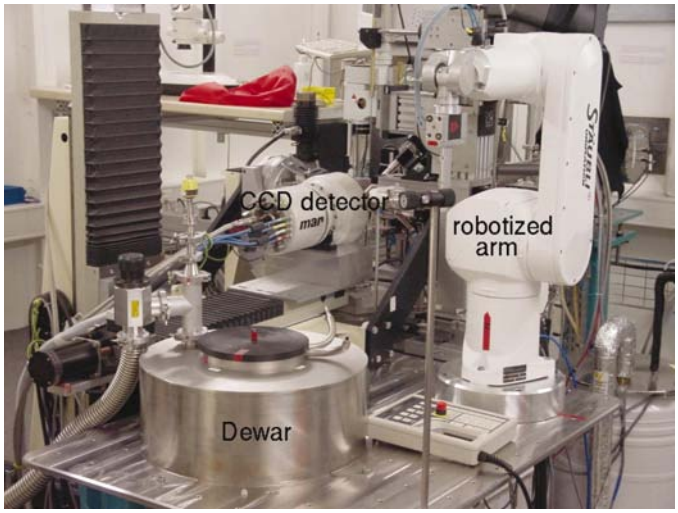

Figure 2
The Cryogenic Automated Transfer System (CATS): a sample changer developed on FIP-BM30A, based on a RX-60L robot from Stäubli (Faverge, France).

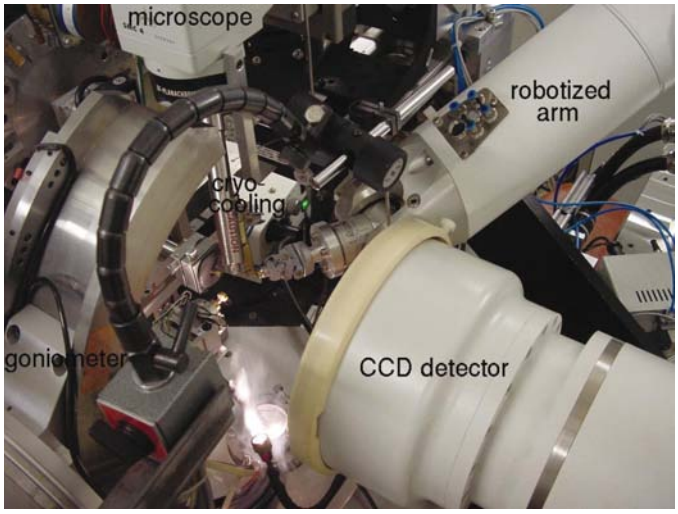

Figure 3
Sample environment, including microscope (upper left) and sample cryocooling (vertical tube in the centre of the image).

Table 3
Statistics of the various data sets collected.

A classical diffractometer was used for the three first data collections (i), (ii) and (iii). The others were performed with the robotic arm. Synchronization of the X-ray shutter and the sample rotation was performed either by sending an electrical signal to the two devices ('external synchronization'; data sets iv, v, vi and vii) or with the shutter being 'controlled by the robot' (data sets viii and ix).

Data collection	Sample	Resolution	Redundancy	Completeness	R_{sym}†	R_{merge}†	R_{free}†
(i) Diffractometer	lys1	2.54	6.8	98.8	2.6		26.3
(ii) Diffractometer ($\alpha = 30^\circ$)	lys1	2.54	6.7	86.2	3.6	2.3	25.4
(iii) Diffractometer	lys2	2.54	6.6	98.3	3.1		26.9
(iv) Robot, high acceleration, single axis, external synchronization	lys2	2.54	5.3	95.8	5.5	5.7	26.3
(v) Robot, high acceleration + off-axis oscillation, external synchronization	lys2	2.54	5.2	95.9	4.3	5.5	26.0
(vi) Robot, low acceleration, external synchronization	chs	1.96	4.2	87.7	8.2		
(vii) Robot, high acceleration, external synchronization	chs	1.96	4.2	87.7	8.1		
(viii) Robot, shutter controlled by the robot	chs	1.96	4.3	87.7	7.7		
(ix) Robot, shutter controlled by the robot + backslash	chs	1.96	4.2	88.2	7.9		

† $R_{sym} = \sum |I_h - \langle I_h \rangle| / \sum I_h$, where $\langle I_h \rangle$ is the average intensity over symmetry-equivalent reflections. R_{merge} is the same comparison between two data sets, data sets (i) and (iii) being the references for crystals lys1 and lys2, respectively. R_{free} is the agreement between measured structure factors and calculated structure factors based on an atomic model (PDB code 193l) after one rigid-body refinement using *CNS* (Brünger *et al.*, 1998) and one cycle of TLS refinement using *REFMAC* (Winn *et al.*, 2001).

which presents optical properties that are very close to those of the crystal, therefore providing very low contrast. We have found that the use of UV light can help in interpreting these types of images. The tests we have performed (Fig. 4) using a 355 nm UV laser installed on the CryoBench at ESRF (Bourgeois *et al.*, 2002) show that fluorescence of aromatic residues in the visible wavelength range significantly improves the contrast with respect to classical light.

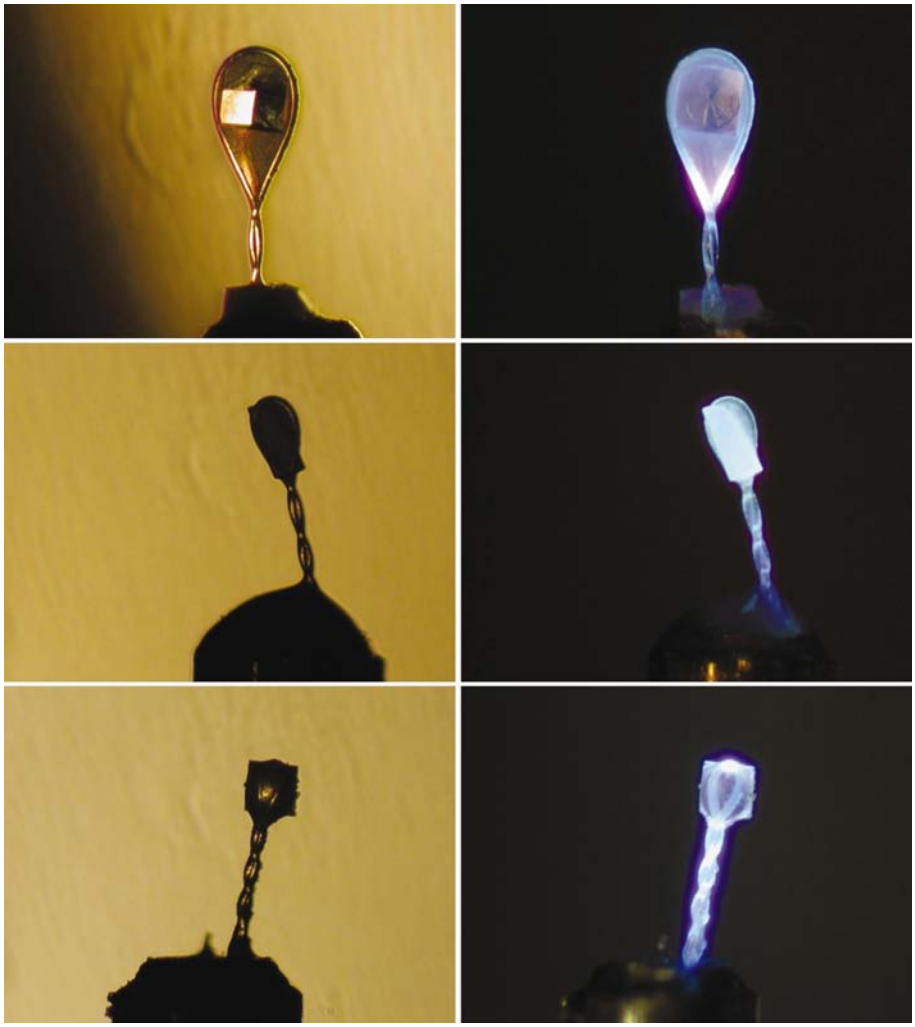

Figure 4
Three protein crystals observed in visible (left) and UV (right) light. The benefit of UV light for sample viewing depends on the aromatic residue content of the protein.

4.3. Quality of data collected

Owing to crystal degradation during irradiation, three different protein crystals were used for the tests: a chalcone synthase crystal (chs; 100 × 200 µm, space group $P3_121$, unit-cell parameters $a = 97.6$, $b = 97.6$, $c = 65.5$ Å; Ferrer *et al.*, 1999) and two lysozyme crystals (named lys1 and lys2; 200 × 200 µm, space group $P4_12_11$, unit-cell parameters $a = b = 77.6$, $c = 36.9$ Å). These crystals were mounted on a loop at the end of the pin of a Hampton magnetic cap. The samples were transferred to the cold stream with a Hampton Cryo-Tong. Each data set consists of 60–90 diffraction frames collected with 1° rotation and 15 s exposure time. The wavelength of the X-ray beam was 0.98 Å and the beam size was 300 µm in diameter. Data were then reduced with the program package *XDS* (Kabsch, 1988, 1993). The quality of the different data sets were evaluated by calculating the R_{sym} factor. This gives an estimation of the data internal coherence by comparing the intensities of symmetry-equivalent reflections.

In order to separate the different parameters contributing to the data quality, several data sets were collected (see Table 3). Since using the microscope and the sample cryocooling already installed on our diffractometer imposes a spindle axis that is not perpendicular to the beam, an initial comparison was carried out with our goniometer. Two data sets were collected on sample lys1: (i) a classical data collection with the spindle axis horizontal (y axis) and perpendicular to the X-ray beam (x axis; Fig. 5*a*) and (ii) a data collection with the spindle axis horizontal, but with a 30° angle with the y axis (Fig. 5*b*). This induced a slight increase in the overall $R_{\rm sym}$.

The accuracy of the spindle rotation is demonstrated by the comparison of the quality of a data set from lysozyme crystal lys2 (iii) recorded on our diffractometer with a data set collected in a similar way with the arm in two different geometries: (iv) using only the last rotation axis, at the end of the robotic arm, as a spindle axis, simulating a classical single-axis goniometer, the sample being centred on this axis with a mechanical goniometer head (Fig. 5*c*), and (v) with the robotic arm combining the six-axis motion in order to keep the crystal in the beam and rotate it around an arbitrary axis (Fig. 5*d*), at the same time replacing a goniometer with sample orientation capability and a motorized goniometer head.

For the 'single-axis' geometry, we tested several ways to synchronize the robot with the shutter and the detector using the chs sample (vi)–(vii). The first method (vi) consists of sending a TTL signal simultaneously to the shutter and the robot. Upon reception of the signal, the robot starts its rotation. In a second method (viii), the robot sends the signal to the shutter when starting the rotation; in a third method (ix), the robot moves backwards to compensate for backlash, starts a large rotation and sends the signal to the shutter when it passes the starting angle of the rotation.

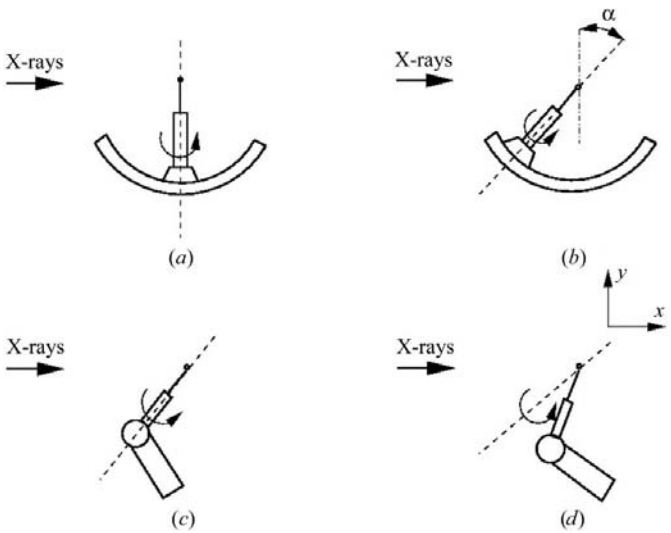

Figure 5
Top view of the different geometries used for data collection: spindle axis of the goniometer perpendicular to the X-ray beam (*a*) or rotated by $\alpha = 30°$ with respect to the vertical direction (*b*), last axis of the robotic arm used as a spindle axis (*c*) or all axes combined to perform an oscillation with respect to an arbitrary axis (*d*).

Comparison of the statistics of all these data collections, with different geometries and modes of synchronization, did not show any significant difference in the quality of the data sets (Table 3). The comparison of the two data sets collected with the lys1 crystal show that the geometrical constraints of an oscillation axis which is not perpendicular to the beam do not significantly alter the quality of data collected. The comparison of the quality of the atomic model refinement with the data collected on the lys2 crystal show that, whatever the geometry, oscillations driven by the robot provide adequate data. The small degradation in the 'single-axis' mode can be attributed to the lower angular accuracy of the last axis (2.75 mdeg) of the robotic arm compared with the other axes (0.72–1.18 mdeg). The slightly higher $R_{\rm merge}$ value can be attributed to the completely different orientation of the crystal when transferred from the goniometer (data set iii) to the robotic arm (data sets iv and v). The data collected using the chs crystal show that the synchronization mode does not affect the quality of data, but that the results are slightly better when the shutter is controlled by the robot. This conclusion is based on the $R_{\rm sym}$ factor, which compares intensity over symmetry-equivalent reflections. This comparison is very sensitive to synchronization and rotation regularity. A 15 s exposure time was used for these tests for 1° oscillation. Slower oscillation speed is not a problem, as the motions of the robotic arm are driven by DC motors. Short exposure time may be problematic, as our shutter (Uniblitz, manufactured by Vincent Associates) is not accurate enough: considering the shutter opening and closing time (total 2 ms), exposures as short as 0.2 s may generate a 1% error in recorded intensities, which is significant at low resolution. Therefore, on FIP-BM30A, we usually do not use an exposure time shorter than 1 s.

5. Conclusions

The tests we performed demonstrate the capability of a robotic arm to replace the goniometer, the goniometer head and the sample changer of a standard setup without degradation of the quality of data collected. The robotic arm can be used for all tasks related to sample handling on a synchrotron station devoted to macromolecular crystallography. Some minor changes, such as a reduced size of the arm and better motion control, may even improve the accuracy, making it suitable for beamlines with smaller beam size and higher flux (*i.e.* requiring shorter exposure time) than the arm we used for these tests. Further integration is still possible, including cryocooling in the arm or also using the robotic arm for beam monitoring. The quality of data collected with this new setup is comparable to that obtained with a classical goniometer and therefore demonstrates the effectiveness of the system.

Macromolecular crystallography is now changing rapidly owing to the opening up of this technique to non-crystallographers and to the increasing demand for synchrotron beamtime resulting from industrial post-genomic projects. This makes the evolution toward simpler and cheaper setups with high reliability necessary. This new experimental setup will bring the required improvement in simplicity, reliability

and cost to future beamlines. It may be an important breakthrough in a context where macromolecular crystallography experiments become routine. It also makes possible the addition at low cost of macromolecular crystallography capabilities to any existing beamline that delivers a monochromated focused beam, whatever the existing equipment.

We thank the staff of CNRS/SERAS (Grenoble) for their technical help and Max Nanao at the IBS (Grenoble) for his careful proofreading.

References

Abola, E., Kuhn, P., Earnest, T. & Stevens, R. C. (2000). *Nature Struct. Biol.* **7**, 973–977.
Bourgeois, D., Vernède, X., Adam, V., Fioravanti, E. & Ursby, T. (2002). *J. Appl. Cryst.* **35**, 319–326.
Brünger, A. T., Adams, P. D., Clore, G. M., DeLano, W. L., Gros, P., Grosse-Kunstleve, R. W., Jiang, J.-S., Kuszewski, J., Nilges, M., Pannu, N. S., Read, R. J., Rice, L. M., Simonson, T. & Warren, G. L. (1998). *Acta Cryst.* D**54**, 905–921.
Burroughs, J. N., Grimes, J. M., Mertens, P. P. C. & Stuart, D. I. (1995). *Virology*, **210**, 217–220.
Cohen, A. E., Ellis, P. J., Miller, M. D., Deacon, A. M. & Phizackerley, R. P. (2002). *J. Appl. Cryst.* **35**, 720–726.
Cusack, S., Belrhali, H., Bram, A., Burghammer, M., Perrakis, A. & Riekel, C. (1998). *Nature Struct. Biol.* **5**, 634–637.
Earnest, T., Snell, G., Cork, C., Meigs, G., Nordmeyer, R., Cornell, E., Yegian, D. & Jin, J. (2002). *Acta Cryst.* **A**58 (Supplement), C56.
Ferrer, J.-L., Jez, J. M., Bowman, M. E., Dixon, R. A. & Noel, J. P. (1999). *Nature Struct. Biol.* **6**, 775–784.
Garman, E. F. & Schneider, T. R. (1997). *J. Appl. Cryst.* **30**, 211–237.
Kabsch, W. (1988). *J. Appl. Cryst.* **21**, 67–71.
Kabsch, W. (1993). *J. Appl. Cryst.* **26**, 795–800.
La Fortelle, E. de & Bricogne, G. (1997). *Methods Enzymol.* **276**, 472–494.
McPhillips, T. M., McPhillips, S. E., Chiu, H.-J., Cohen, A. E., Deacon, A. M., Ellis, P. J., Garman, E., Gonzalez, A., Sauter, N. K., Phizackerley, R. P., Soltis, S. M. & Kuhn, P. (2002). *J. Synchrotron Rad.* **9**, 401–406.
Muchmore, S. W., Olson, J., Jones, R., Pan, J., Blum, M., Greer, J., Merrick, S. M., Magdalinos, P. & Nienaber, V. L. (2000). *Structure*, **8**, 243–246.
Ohana, J., Jacquamet, L., Joly, J., Bertoni, A., Taunier, P., Michel, L., Charrault, P., Pirocchi, M., Carpentier, P., Borel, F., Kahn, R. & Ferrer, J.-L. (2004). *J. Appl. Cryst.* **37**, 72–77.
Olson, J. A., Jones, R. B., Nienaber, V. L., Muchmore, S. W., Pan, J. Y. & Greer, J. (2002). US Patent Application 20 020 126 802.
Peat, T., de La Fortelle, E., Culpepper, J. & Newman, J. (2002). *Acta Cryst.* D**58**, 1968–1970.
Roth, M., Carpentier, P., Kaïkati, O., Joly, J., Charrault, P., Pirocchi, M., Kahn, R., Fanchon, E., Jacquamet, L., Borel, F., Bertoni, A., Israel-Gouy, P. & Ferrer, J.-L. (2002). *Acta Cryst.* D**58**, 805–814.
Teng, T.-Y. & Moffat, K. (1998). *J. Appl. Cryst.* **31**, 252–257.
Terwilliger, T. C. & Berendzen, J. (1999). *Acta Cryst.* D**55**, 849–861.
Winn, M., Isupov, M. & Murshudov, G. N. (2001). *Acta Cryst.* D**57**, 122–133.